

# Performance and Limitations of Quasi-Phase Matching Semiconductor Waveguides with Picosecond Pulses

Sean J. Wagner<sup>a</sup>, S. Chaitanya Kumar<sup>b</sup>, Omid Kokabee<sup>b</sup>, Barry M. Holmes<sup>c</sup>, Usman Younis<sup>c</sup>,  
Majid Ebrahim Zadeh<sup>b</sup>, David C. Hutchings<sup>c</sup>, Amr S. Helmy<sup>a</sup>, and J. Stewart Aitchison<sup>a</sup>

<sup>a</sup>Edward S. Rogers Sr. Department of Electrical and Computer Engineering,  
University of Toronto, 10 King's College Road, Toronto, Ontario, M5S 3G4, Canada;

<sup>b</sup>ICFO - Institut de Ciències Fòtonique, Mediterranean Technology Park, 08860 Castelldefels,  
Barcelona, Spain;

<sup>c</sup>Department of Electronics and Electrical Engineering, University of Glasgow, Glasgow,  
G12 8QQ Scotland, UK

## ABSTRACT

Quasi-phase matched (QPM) second-order nonlinear optical processes in compound semiconductors are attractive for frequency conversion because of their large nonlinear susceptibilities and their mature fabrication processes that permit monolithic integration with pump lasers and other optical elements. Using quantum well intermixing (QWI), we have fabricated domain-disordered QPM (DD-QPM) waveguides in GaAs/AlGaAs superlattices and have previously demonstrated continuous-wave (CW) Type-I second-harmonic generation (SHG) and pulsed Type-II SHG. CW experiments were complicated by Fabry-Perot resonances and thermal bistability. Experiments using a 2-ps pulsed system were affected by third-order nonlinear effects, group-velocity mismatch (GVM), and poor spectral overlap with the conversion bandwidth. A better evaluation of the conversion efficiency may, however, be determined by using longer pulses in order to avoid these complications. By this, the effective CW conversion efficiency and  $\chi^{(2)}$  modulation can be ascertained. In this paper, we demonstrate SHG in DD-QPM waveguides with reduced parasitic effects by using 20 ps pulses. The waveguide structure consisted of a core layer of GaAs/Al<sub>0.85</sub>Ga<sub>0.15</sub>As superlattice into which QPM gratings with a period of 3.8  $\mu\text{m}$  were formed using QWI by As<sup>2+</sup> ion implantation. For a Type-I phase matching wavelength of 1583.4 nm, average second-harmonic (SH) powers produced were as high as 2.5  $\mu\text{W}$  for 2 ps pulses and 3.5  $\mu\text{W}$  for 20-ps pulses. At low input powers, the SHG average power conversion efficiency of the 2-ps system was more than 10 times larger than the 20 ps system. As power was increased, the SH power saturated and conversion efficiency decreased to nearly equal to the 20-ps system which remained consistent over the same power range. This is attributed to a reduction in third-order nonlinear effects, a smaller pulse spectral width that overlaps better with the conversion bandwidth, and less pulse walkoff for the 20-ps pulses. Thus, by using 20-ps pulses over 2-ps pulses, we achieved similar output SH powers and potentially higher SH powers are possible since there was no observed saturation at high input power.

**Keywords:** Quasi-phase matching, semiconductor superlattice, quantum well intermixing, second-harmonic generation, monolithic integration

## 1. INTRODUCTION

Second-order nonlinear optical processes in compound semiconductors are attractive for frequency conversion. In particular, AlGaAs has been widely considered as a second-order nonlinear material because of its large nonlinear susceptibilities, mature fabrication processes, wide transparency range into the midinfrared, and the potential

---

Send correspondence to S. J. Wagner: sean.wagner@utoronto.ca

to directly integrate pump laser diodes onto the same chip. However, unlike bulk nonlinear crystals, AlGaAs is linearly isotropic and thus phase matching is challenging. Several methods have been studied to overcome this limitation including modal phase matching,<sup>1</sup> artificial form birefringence in AlGaAs/Al<sub>x</sub>O<sub>y</sub> waveguides,<sup>2</sup> and orientation-patterned GaAs.<sup>3</sup> However, these schemes are not amenable to integration with a pump laser and are limited by inherently high linear loss. Thus, creating a monolithically integrated and efficient optical frequency conversion device is somewhat challenging using these methods.

We have been exploring an approach to phase matching using a GaAs/AlGaAs superlattice platform and quantum-well intermixing (QWI).<sup>4</sup> By using QWI, we have fabricated waveguides in which the nonlinear susceptibility  $\chi^{(2)}$  is periodically suppressed in GaAs/AlGaAs superlattices thus forming a domain-disordered quasi-phase matched (DD-QPM) grating. Such structures are formed by readily available lithographic processes, have potentially low linear loss, and are compatible with pump laser integration. Second harmonic generation (SHG) has been demonstrated using DD-QPM waveguides in recent years with increasing efficiency as progressive improvements have been made in device design and fabrication processes.<sup>5-7</sup> Also, we have demonstrated difference frequency generation using such waveguides.<sup>8</sup> However, efficiencies were below expected, which was the result of parasitic effects including third-order nonlinearities when using ultrafast laser systems<sup>9</sup> and bistability when using continuous wave laser systems.<sup>7</sup> Thus, a new operating regime may provide an appropriate balance and yield better conversion efficiency. In this paper, we report on SHG results in DD-QPM waveguides using a 20-ps pulse source and a 2-ps pulse source. From the measured results, the performance in each regime is evaluated and the limitations of using such pulses is examined.

## 2. BACKGROUND

In early work with DD-QPM superlattice waveguides, SHG was achieved using ultrafast laser systems with pulse lengths on the order of 250 fs.<sup>5</sup> While second harmonic powers reached over 1  $\mu$ W, conversion efficiency was low. One reason for this was that the spectral width of the 250 fs pulses was five times larger than the acceptance bandwidth of the QPM device. Thus, large portions of the source spectrum were not phase matched. This was resolved by moving to 2-ps pulse systems, which have pulse spectral widths of about ten times smaller than 250 fs systems. Improved conversion efficiency was achieved,<sup>6</sup> however linear losses due to fabrication difficulties limited the overall SHG process.

Recently, we were able to improve the fabrication processes for DD-QPM superlattice waveguides such that the linear losses were low enough to demonstrate continuous-wave SHG.<sup>7</sup> However, measurements of the conversion efficiency were complicated by the Fabry-Perot resonances of the waveguide and by thermally-induced optical bistability. Also, the input power had to be kept low in order to avoid catastrophic damage to the waveguides and this limited the second-harmonic power generated to less than 2  $\mu$ W.

We have also achieved Type-II SHG with 2-ps pulses.<sup>9</sup> However, when increasing the input power of the fundamental wavelength, a saturation effect was observed. This effect was caused by the high peak pulse power of the 2-ps pulses which lead to third-order nonlinear effects such as self-phase modulation (SPM) and two-photon absorption (TPA). Furthermore, using short pulses resulted in group-velocity mismatch (GVM). Using computer simulations, we estimated that the resulting walkoff between the fundamental and generated second-harmonic pulse would have reduced the conversion efficiency by about 23%.<sup>10</sup> Lastly, the wide spectrum of 2-ps pulses led to poor overlap with conversion bandwidth of the QPM waveguides. This was evidenced by an over 30% narrowing of the second-harmonic pulse spectrum when on the phase matching wavelength compared to when several nanometers off the phase matching wavelength. Overall, these effects limited the potential second-harmonic power that could be generated.

In order to improve the conversion efficiency, a new temporal excitation scheme needed to be explored. A system producing 20-ps pulses was chosen for several reasons. First, the pulse peak power of a 20-ps system with a similar repetition rate is ten times lower than a 2-ps system for the same average power. Thus, third-order effects should not be induced to significant levels such as to affect the SHG process. Second, the pulse spectral bandwidth of 20-ps pulses should be several times smaller and provide a better overlap with the conversion

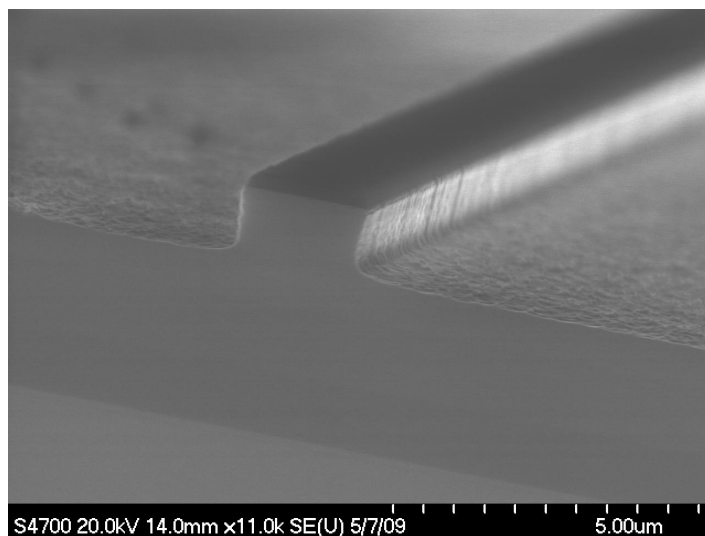


Figure 1. Scanning electron micrograph of a DD-QPM ridge waveguide

bandwidth. Lastly, the walkoff length between the fundamental 20-ps pulses and the generated second-harmonic pulses should be less than the sample length, which is about 1 mm.

### 3. DEVICE FABRICATION

The waveguide structure used here was the same as that in our previous work.<sup>7</sup> It consisted of a 0.6  $\mu\text{m}$ -thick core layer of 14:14 monolayer GaAs/ $\text{Al}_{0.85}\text{Ga}_{0.15}\text{As}$  superlattice. Buffer layers of 300 nm-thick  $\text{Al}_{0.56}\text{Ga}_{0.60}\text{As}$  were placed on either side of the core to expand the optical mode profile and improve optical coupling efficiency. The cladding layers were 800 nm-thick and composed of  $\text{Al}_{0.60}\text{Ga}_{0.40}\text{As}$ . A 1000 nm-thick isolation layer of  $\text{Al}_{0.85}\text{Ga}_{0.15}\text{As}$  was added below the lower cladding layer to prevent optical leakage to the substrate. A 100 nm cap layer of GaAs was added to the surface of the wafer to prevent oxidation of the wafer. All layers were grown by molecular beam epitaxy on a semi-insulating GaAs substrate.

QPM gratings with several periods and different drawn duty cycles were formed in the superlattice using QWI. First, a thin gold layer was deposited onto a dielectric-coated sample via sputtering. PMMA was then spun onto the wafer and patterned with the grating via electron beam lithography (EBL). After development, a 2.0  $\mu\text{m}$ -thick gold mask was grown by electroplating. This was followed by  $\text{As}^{2+}$  ion-implantation through the gold mask, then rapid thermal annealing at 775°C for 60 s. Rib waveguides 3.0  $\mu\text{m}$  wide and 1.3  $\mu\text{m}$  deep were fabricated by EBL and reactive ion etching. The final sample was cleaved to a length of 1 mm. Figure 1 shows a scanning electron micrograph of a DD-QPM ridge waveguide. Linear loss coefficients averaging 2.5  $\text{cm}^{-1}$  in value were measured around 1550 nm using a narrow linewidth tunable laser and the Fabry-Perot method.

### 4. EXPERIMENTAL SETUP

The setup for the SHG experiment is shown in Figure 2. The 20-ps pulse source was a MgO:PPLN-based optical parametric oscillator (OPO) synchronously pumped by a mode-locked ytterbium-doped fiber laser emitting at 1064 nm.<sup>11</sup> Pulses were emitted at a repetition rate of 81 MHz with average powers of up to 300 mW for wavelengths around 1600 nm. Wavelength tuning was achieved by changing the temperature of the MgO:PPLN crystal and OPO cavity length. The pulse spectral width was measured as 0.47 nm. For the experiments with shorter pulses, a singly-resonant CTA-based OPO synchronously pumped by a mode-locked Ti:saph laser was used. Pulses were 2-ps in length at a repetition rate of 75.6 MHz and had average powers of up to 250 mW. Pulses were nearly transform limited having spectral widths of 2-3 nm.

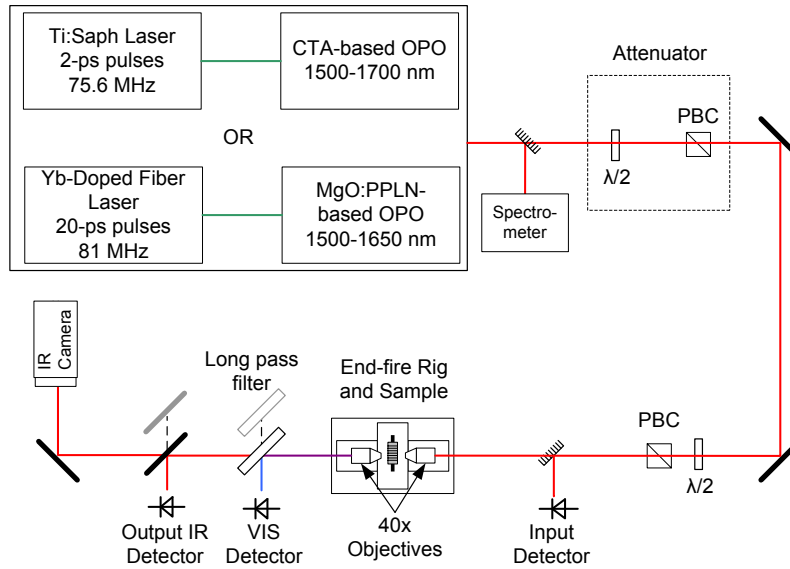


Figure 2. Schematic of the experimental setup for second-harmonic generation with DD-QPM superlattice waveguides. The source laser system was either the Ti:sapphire/OPO system for 2-ps pulses or the Yb fiber laser/OPO system for 20-ps pulses.

A waveplate and polarizing beam cube was used to set the input polarization to horizontal which corresponded to the TE polarization for the ridge waveguides. This excited the Type-I SHG process (TE fundamental in, TM second-harmonic out). Light was coupled into and out of the waveguides using the end-fire technique with 40× objective lenses. The output fundamental and second-harmonic wavelengths from the QPM sample were split using a long-pass filter and directed onto separate photodetectors.

## 5. RESULTS AND ANALYSIS

The phase matching wavelength in a waveguide with a 3.8 μm QPM period was found at 1583.5 nm. Output second-harmonic powers were as high as 2.5 μW for the 2-ps system with 131 mW input at the waveguide facet, and 3.5 μW for the 20-ps system with 165 mW input. Accounting for the facet reflectivities (26%) and the input coupling efficiency yields internal power levels for the waveguide. From here, the internal *average power normalized conversion efficiency* can be found which is defined as

$$\bar{\eta} = \frac{\overline{P_{2\omega}}}{\overline{P_{\omega}}^2 L^2} \times 100\% \quad (1)$$

where  $\overline{P_{2\omega}}$  and  $\overline{P_{\omega}}$  are the second-harmonic and fundamental average powers and  $L$  is the waveguide length. Using this, the normalized conversion efficiencies were 27 %W<sup>-1</sup>cm<sup>-2</sup> for the 20-ps pulses and 24 %W<sup>-1</sup>cm<sup>-2</sup> for the 2-ps pulses at high power. Under ideal circumstances, the 2-ps system should have produced much higher average power conversion efficiency since the peak pulse power is over 10 times larger than the 20-ps system. However, this is not the case as both efficiencies are nearly equal.

Another way to examine this result is to normalize the conversion efficiency by the pulse length. Assuming a Gaussian pulse shape, Equation 1 can be reformulated to give the *effective instantaneous conversion efficiency*

$$\eta_{\text{eff}} = T_0 f \sqrt{\pi \bar{\eta}} \quad (2)$$

where  $T_0$  is the 1/e pulse half-width and  $f$  is the pulse repetition rate. By this measure, the 20-ps pulses yielded conversion efficiencies ten times larger than the 2-ps pulses when at average internal input powers above 50 mW.

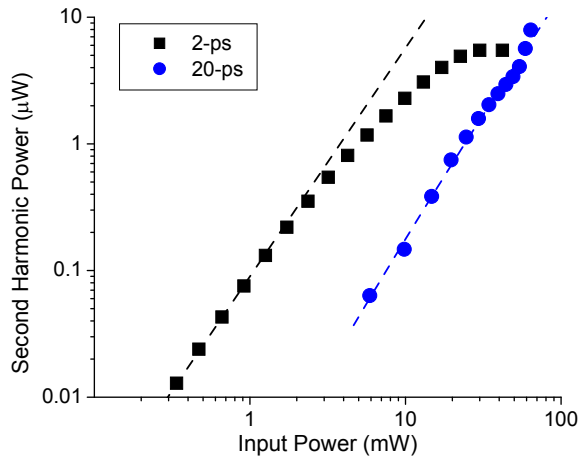


Figure 3. Output internal second-harmonic powers generated versus internal input power on a log-log scale. Dashed lines represent the best fit slope.

This is evidence that parasitic effects disrupted the phase matching process more predominantly in the 2-ps pulse because of the higher peak powers and wider spectral width.

For both pulse durations, we investigated how the output second harmonic scales with input power. The resulting measurements are shown in Figure 3 along with best linear fits for the log-log scale. At low powers, the 2-ps system produced output second harmonic powers over a magnitude larger than in the 20 ps case, as was expected. At larger powers, the output second harmonic power saturates for the 2-ps case. Beyond internal input powers of 30 mW, little or no increase was observed in the generated second-harmonic. Thus, the 2-ps system was limited in usability to powers less than this. In contrast, second-harmonic power steadily increased in the 20-ps system without saturation at high powers. The slope of the 20-ps curve also had a slope on the log-log plot that was 1.95 compared with 1.80 for the 2-ps system. Thus, the second-harmonic power generated by the 20-ps pulses showed an input power dependence more consistent with the quadratic relationship of an SHG process.

Figure 4 shows how the conversion efficiency changes with input power. For the 20-ps case, the conversion remains steady around a mean value of  $23 \%W^{-1}cm^{-2}$  over the span of 50 mW of input power. This is over an order of magnitude lower than the 2-ps case at low power where the conversion efficiency is nearly  $365 \%W^{-1}cm^{-2}$ . However, as the power is increased, the conversion efficiency drops to  $31 \%W^{-1}cm^{-2}$ , which is similar value to the 20-ps system. Both the saturation in the second-harmonic power and the reduced conversion efficiency show that the 2-ps pulses are strongly affected by SPM and TPA while the 20 ps pulses are relatively unaffected due to their reduced peak power. With the 20-ps system, the conversion efficiency is expected to remain consistent at larger input powers. Assuming this, extrapolating the best fit line of Figure 3 to high input powers, using 20-ps pulses could possibly generate greater second-harmonic powers of several 10's of microwatts. However, third-order effects are expected become strong enough to disrupt the SHG process for the 20-ps system with input average powers over 200 mW in a similar manner as the 2-ps system.

## 6. CONCLUSIONS

In conclusion, we have measured and compared second-harmonic generation in DD-QPM semiconductor waveguides using a 2-ps pulse source and 20-ps pulse source. The 2-ps system suffered from SPM at high power and poor spectral overlap with the conversion bandwidth. This reduced the conversion efficiency and limited the output second-harmonic power to a few microwatts. These effects were significantly reduced in the 20-ps case

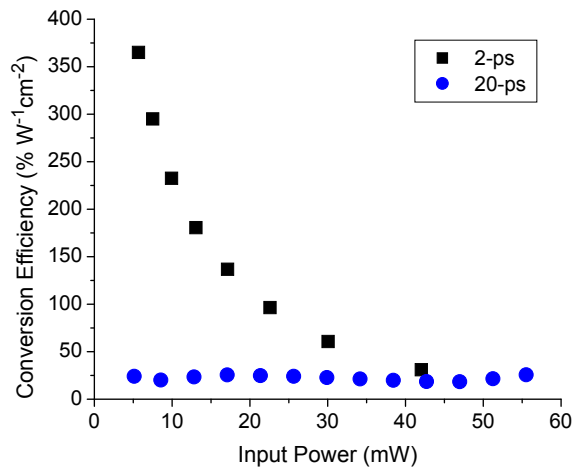


Figure 4. Normalized internal conversion efficiency versus internal input power

such that the conversion efficiency remained consistent as the input power was changed. In this regard, the 20-ps case provided better conversion efficiency at high power and should allow operation at even higher powers.

## ACKNOWLEDGMENTS

Thank you to the staff at the James Watt Nanofabrication Facility at the University of Glasgow and to the staff at the Surrey Ion Beam Centre at the University of Surrey for microfabrication services. Funding was provided by EPSRC, NSERC, ICFO, and the Ontario Centre's of Excellence (OCE).

## REFERENCES

1. K. Moutzouris, S. V. Rao, M. Ebrahimzadeh, A. De Rossi, M. Calligaro, V. Ortiz, and V. Berger, "Second-harmonic generation through optimized modal phase matching in semiconductor waveguides," *Appl. Phys. Lett.* **83**(4), pp. 620–622, 2003.
2. K. Moutzouris, S. V. Rao, M. Ebrahimzadeh, A. D. Rossi, V. Berger, M. Calligaro, and V. Ortiz, "Efficient second-harmonic generation in birefringently phase-matched GaAs/Al<sub>2</sub>O<sub>3</sub> waveguides," *Opt. Lett.* **26**(22), pp. 1785–1787, 2001.
3. T. Skauli, K. L. Vodopyanov, T. J. Pinguet, A. Schober, O. Levi, L. A. Eyres, M. M. Fejer, J. S. Harris, B. Gerard, L. Becouarn, E. Lallier, and G. Arisholm, "Measurement of the nonlinear coefficient of orientation-patterned GaAs and demonstration of highly efficient second-harmonic generation," *Optics Letters* **27**(8), pp. 628–630, 2002.
4. J. H. Marsh, "Quantum well intermixing," *Semi. Sci. Tech.* **6**, pp. 1136–1155, 1993.
5. K. Zeaier, D. C. Hutchings, R. M. Gwilliam, K. Moutzouris, S. V. Rao, and M. Ebrahimzadeh, "Quasi-phase-matched second-harmonic generation in a GaAs/AlAs superlattice waveguide by ion-implantation-induced intermixing," *Opt. Lett.* **28**(11), pp. 911–913, 2003.
6. D. C. Hutchings, M. Sorel, K. Zeaier, A. J. Zilkie, B. Leesti, A. S. Helmy, P. W. E. Smith, and J. S. Aitchison, "Quasi-phase-matched second harmonic generation with picosecond pulses in GaAs/AlAs superlattice waveguides," in *Proceedings Nonlinear Guided Waves*, OSA, (Toronto, Canada), 2004.
7. S. J. Wagner, B. M. Holmes, U. Younis, A. S. Helmy, J. S. Aitchison, and D. C. Hutchings, "Continuous wave second-harmonic generation using domain-disordered quasi-phase matching waveguides," *Applied Physics Letters* **94**(15), pp. 151107–3, 2009.

8. S. J. Wagner, I. Sigal, A. S. Helmy, J. S. Aitchison, U. Younis, B. M. Holmes, and D. C. Hutchings, "Difference frequency generation in domain-disordered quasi-phase matching semiconductor waveguides," in *Conference on Lasers and Electro-Optics*, OSA, (San Jose, CA), 2010.
9. D. C. Hutchings, S. J. Wagner, B. M. Holmes, U. Younis, A. S. Helmy, and J. S. Aitchison, "Type-II quasi-phase matching in periodically intermixed semiconductor superlattice waveguides," *Optics Letters* **35**(8), pp. 1299–1301, 2010.
10. S. J. Wagner, A. Al Mehairi, J. S. Aitchison, and A. S. Helmy, "Modeling and Optimization of Quasi-Phase Matching via Domain-Disordering," *IEEE Journal of Quantum Electronics* **44**(5), pp. 424–429, 2008.
11. O. Kokabee, A. Esteban-Martin, and M. Ebrahim-Zadeh, "High-power, fiber-laser-pumped picosecond optical parametric oscillator for the near- to mid-infrared," in *Conference on Lasers and Electro-Optics*, OSA, (San Jose, CA), 2010.